Effects of speed reduction in climb, cruise and descent phases to generate linear holding at no extra fuel cost

Yan Xu Ramon Dalmau Xavier Prats
Technical University of Catalonia
Castelldefels, Barcelona (Spain)

***Abstract*—Speed reduction strategies have proved to be useful to recover delay if air traffic flow management regulations are cancelled before initially planned. Considering that for short-haul flights the climb and descent phases usually account for a considerable percentage of the total trip distance, this paper extends previous works on speed reduction in cruise to the whole flight. A trajectory optimization software is used to compute the maximum airborne delay (or linear holding) that can be performed without extra fuel consumption if compared with the nominal flight. Three cases are studied: speed reduction only in cruise; speed reduction in the whole flight, but keeping the nominal cruise altitude; and speed reduction for the whole flight while also optimizing the cruise altitude to maximize delay. Three representative flights have been simulated, showing that the airborne delay increases significantly in the two last cases with nearly 3-fold time for short-haul flights and 2-fold for mid-hauls with the first case. Results also show that fuel and time are traded along different phases of flight in such a way the airborne delay is maximized while the total fuel burn is kept constant.**

I. INTRODUCTION

With the continuous growth of air transportation industry, air traffic flow management (ATFM) has become crucial to prevent airport and airspace capacity-demand imbalances while enabling airlines to operate safe and efficient flights. In the majority of the situations, ATFM regulations are issued due to weather related capacity reductions. Considering the uncertainties in weather prediction and other unforeseen factors, ATFM decisions are typically conservative and the planned regulations may last longer than actually needed [1], [2]. At present, ground delay is more preferable than airborne delay (holding) from a safety, environmental and operating cost points of view. However, when regulations are cancelled before their initial planned ending time, as occur often [3], [4], the already accomplished delay on ground cannot be recovered, or can be partially recovered by increasing speed, leading to extra fuel consumption.

In order to overcome this issue, a speed reduction (SR) strategy was proposed in [5], which aimed at partially absorbing ATFM delays airborne. Ground delayed aircraft were enabled to fly at the minimum fuel consumption speed (typically slower than nominal cruise speed initially chosen by the airline) performing in this way some airborne delay, at the same time fuel was saved with respect than the nominal flight. This strategy was further explored in [6], where aircraft were allowed to cruise at the lowest possible speed in such a way the specific range (i.e. the distance flown per unit of fuel consumption) remained the same as initially planned. In this situation, if regulations were cancelled, aircraft already airborne and flying slower, could increase their cruise speed to the initially planned speed and recover part of the delay without extra fuel consumption [2], [6]–[8].

As a wider concept of SR, the speed control (SC) strategies have proven successful for several ATFM scenarios. For instance, in [9], en-route SC was proposed to prevent aircraft from performing airborne holding patterns when arriving at a congested airspace. In [10], aircraft were required to reduce their speed to avoid arriving at the airport before its opening time to reduce unnecessary holdings. Congestion problems at sector level were resolved by controlling the speed with 10% intervals [11]. Some research has also been conducted considering speed control as an additional decision variable to solve the ground holding problem [12].

The SC strategies could be applied to different flight phases as an effective mean to manage air traffic. Although previous works mainly focused on the cruise phase of flight, many studies have been also conducted for the implement of SC strategies in terminal manoeuvring area (TMA). For instance, in [13], where descent speed control was introduced for conflict resolution and analysed by means of Monte Carlo simulations. In [14] the time-based concept using climb and descent SC, as well as flight path control, proved to be efficient for TMA traffic management. Finally, according to [15], half of the TMA inefficiency could be recovered by means of SC whilst maintaining runway capacity.

In this paper, the SR strategy proposed in [6] is extended in such a way that not only the cruise phase is used to perform linear holding, but also the climb and descent phases are subject of optimisation to maximize the total amount of airborne delay that can be done without incurring extra fuel consumption. With the speed adjusted in climb and descent, constraints of terminal area may arise, such as the need to organize traffic for instance. However, these tactical ATM constraints, as were discussed in detail in [16], [17], are out of the scope of this paper.

This paper is outlined as follows: in Sec. II the research background are introduced with regard to implement the SR strategy in different flight phases. Sec. III presents the experimental setup, including a general description of the trajectory

optimization tool. In Sec. IV the results are discussed and finally, the conclusions are presented in Sec. V.

II. SPEED REDUCTION FOR ATFM

Current on-board flight management systems enable airlines to optimize the aircraft trajectory in terms of direct operating costs by means of the cost index (CI), which represents the ratio between time-based cost and the cost of fuel [18]. The higher the CI is, the more importance will be given to the trip time and the faster the optimal aircraft speed will be. Along with the CI, aircraft payload, flight distance, and weather conditions determine the optimal cruise flight level and Mach along with the climb and descent profiles.

In this paper, optimal trajectories computed with a given CI would be regarded as the nominal flights, and labelled as Case-0. Based on Case-0, different speed reduction (SR) strategies will be analysed, denoted by Case-1, Case-2 and Case-3.

A. Case-1: SR in cruise maintaining the nominal flight level

Typical operating cruise speeds are higher than the MRC (maximum range cruise) speed (i.e. the speed corresponding to CI=0), since aircraft operators also consider time-related costs when planning their flights. Accordingly, the specific range for cruise is lower than the maximum specific range for that altitude. In [2], [6]–[8] this strategy was already explored and the authors defined the equivalent speed V_{eq}^{crz} as the minimum speed that produces the same specific range as flying at the nominal speed $V_0^{crz} = V_{ECON}^{crz}$, as shown in Fig. 1. Therefore, for all speeds between V_{eq}^{crz} and V_0^{crz}, the fuel consumption will be the same or lower than initially planned while the flight time in cruise will be higher.

The margin between V_0^{crz} and V_{eq}^{crz} is a function of both nominal CI and the shape of the specific range curve, which in turn is aircraft, flight level and weight dependent. Moreover, it is still worth noting that V_{eq}^{crz} might be limited by the minimum operational speed of the aircraft at that given flight level and weight (including possible safety margins). In this paper, the Green Dot (GD) speed is adopted as the minimum bound, which depicts the best lift to drag ratio speed in clean configuration. In manual flight, the selected speed/Mach could

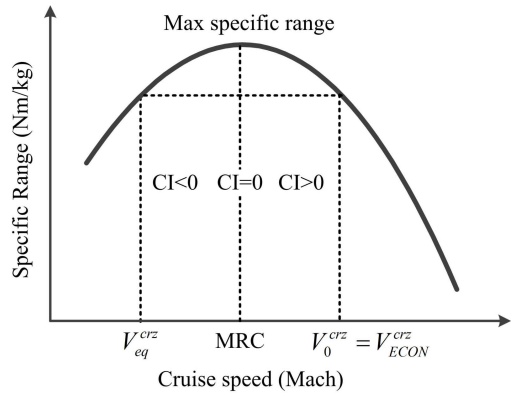

Fig. 1. Specific range as a function of cruise speed.

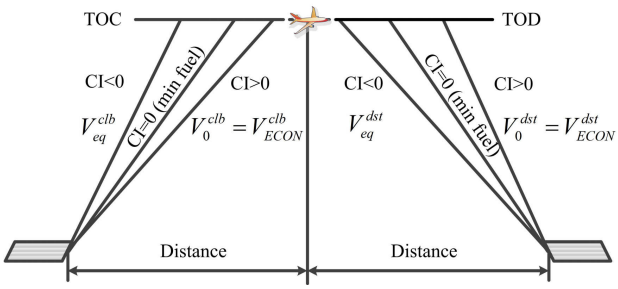

Fig. 2. Climb and descent profiles versus cost index.

be set to V_{LS} (lowest selectable speed, the stalling speed at 1.3g) that is a lower than the GD speed [19]. Yet, considering the operability of the SR strategy and aiming at automatic flight, it is more realistic to choose the managed mode and therefore GD as the lower bound for speed. According to [20] GD speed, below FL200 equals to 2 weight (tons) + 85 (kt), and above FL200, adds 1 kt per 1000ft.

B. Case-2: SR in climb, cruise and descent maintaining the nominal flight level

Not only is the cruise phase affected by CI, but also climb and descent phases. With CI increasing, the speed of both climb and descent increases, as well as fuel consumption, and the climb profile becomes shallower, while conversely the descent profile turns steeper (see Fig. 2) [21].

Thus, the SR strategy could be extended to the whole flight and not just the cruise phase, in order to increase the amount of airborne delay and even make it appealing for short-haul flights, as climb and descent often represent a considerable percentage of the total trip distance. A similar behaviour than in cruise occurs for climb and descent phases when a CI higher than 0 is selected by the operator. In such case, the climb and descent speeds are faster than those of minimum fuel $V_{minfuel}^{clb/dst}$, and there exists an equivalent speed $V_{eq}^{clb/dst}$ yielding the same fuel consumption as $V_0^{clb/dst}$.

For a given aircraft, the theoretical minimal fuel speed for climb $V_{minfuelT}^{clb}$ is not constant and changes with altitude (and with aircraft mass as long as fuel is burnt). This speed is denoted with a green dashed line in Fig. 3, for a hypothetical climb.

In real operations this speed is not followed, due to operational or ATM constraints. Unlike in cruise where flight is performed at a constant Mach number, the climb is divided into several speed segments. These typically include a speed limitation at low altitudes, typically 250kt IAS (indicated airspeed) below FL100, followed by an acceleration to a constant IAS climb, followed by a constant Mach climb above the crossover altitude. Fig. 3 shows an example for such a climb speed profile (250kt/300kt/M0.78 for this example) with a solid black line and denoted in this paper as $V_{minfuel}^{clb}$.

Nominal climb speeds for CI greater than zero will lead to climb speed profiles as shown by the red line V_0^{clb} in

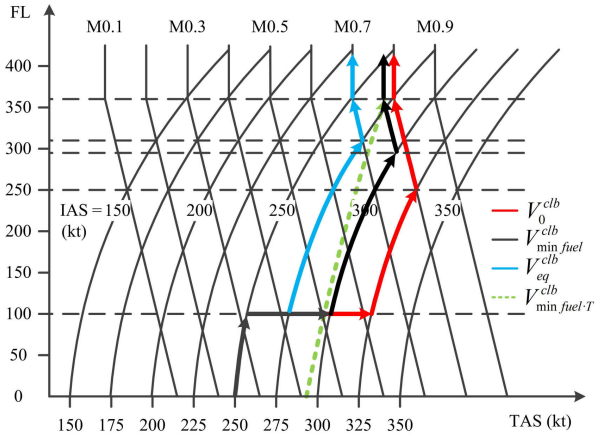

Fig. 3. Speed profiles with convertional operation constraints.

Fig. 4, while V_{eq}^{clb} denotes the equivalent climb speed profile leading to the same fuel consumption. As for descent, the realistic speed profile is just like the one in climb, but with opposite sequence that is from the constant Mach descent above crossover altitude to the deceleration process at low altitudes.

It should be noted that when SR is implemented in climb and descent phases, the minimum speed is also limited by GD.

C. Case-3: SR in climb, cruise and descent and optimising for cruise flight level

In general, as the cruise speed reduces, the optimal flight level decreases. Since the equivalent cruise speed V_{eq}^{crz} is lower than the nominal cruise speed V_0^{crz}, it is possible that the initial planned flight level is no longer the optimal one in the SR cases. When a new flight level exists, by which the specific range keeps the same or higher while speed reduces more, then it could replace the nominal one. Furthermore, if the new flight level decreases, more fuel can be saved for climb and descent due to the reduction in the altitude of the TOC and TOD.

This Case implements the SR strategy in the whole flight (as in Case-2), but allowing to optimise for the best cruise altitudes in such a way that the total airborne delay is maximised, while keeping fuel consumption equal or lower than in the nominal flight (Case-0).

D. Optimisation objective and constraint for the SR strategy

For the SR Cases, consider that the basic optimisation objective and constraint are as follows:

$$max(\sum T_i^{clb} + \sum T_j^{crz} + \sum T_k^{dst}) \tag{1}$$

$$\sum F_i^{clb} + \sum F_j^{crz} + \sum F_k^{dst}) \leq F_{nominal} \tag{2}$$

where *i*, *j*, *k* represent the segments that each phase is divided, which will be further discussed in the following section. T^{clb}, T^{crz}, T^{dst} are the time needed for climb, cruise and descent respectively, and F^{clb}, F^{crz}, F^{dst} denote the fuel consumed for each phase while $F_{nominal}$ is the fuel as initial planned in the nominal flight. Note that for Case-1 T^{clb} and T^{dst} are not subject to optimisation and are fixed to the nominal climb and descent times, respectively.

This makes it clear that in Case-2 and Case-3, the flight as a whole is optimized rather than the climb, cruise or descent phase separately. The above discussions are all based on one specific phase (climb, cruise or descent), and we can tell there exist some trade-off between fuel and time (speed) within each phase (F^{clb} & T^{clb}, F^{crz} & T^{crz}, F^{dst} & T^{dst}). Nevertheless, the trade-off between these three phases (F^{clb} & F^{crz} & F^{dst}, T^{clb} & T^{crz} & T^{dst}) should be considered as well, which may contribute to better results.

III. SIMULATION SETUP

This section introduces the main features of the tool used to generate the trajectories shown in this paper, which is an in-house software capable to optimize trajectories for any phase of flight, allowing to setup a wide range of operational constraints and taking into account different optimization criteria. Simulation procedurals with respect to each of the four Cases of the study are also included in this section.

A. Optimal trajectory generation tool

The main architecture of this trajectory generation tool is shown in Fig. 4. Given a set of inputs, the trajectory generation tool formulates the optimization of trajectory as a multi-phase constrained optimal control problem, in which it is desired to determine the controls of the aircraft (thrust and flight path angle) such that a given cost function is maximized or minimized while satisfying a set of constraints [22]. Further mathematical details on the formulation of optimal control problems for trajectory optimization applications can be found in [23]. The resultant optimal control problem is solved by means of numerical optimization using direct collocation methods, which transform the original continuous (and thus infinite) optimal control problem into a (discrete and finite) nonlinear programming (NLP) optimization problem. The new finite variable NLP problem is solved by using solvers CONOPT (as NLP) and SBB as MINLP (mixed integer nonlinear programming), both bundled into the GAMS software suite.

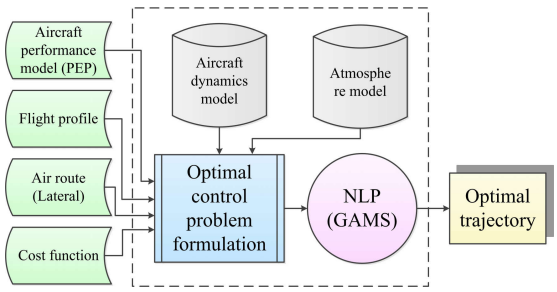

Fig. 4. Main architecture of the optimal trajectory generation tool.

The formulation of the optimal control problem requires mathematical models capturing aircraft dynamics and performances, along with a model for certain atmospheric variables. The equations of motion are derived for a point-mass aircraft model (three degrees of freedom) without winds and assuming continuous vertical equilibrium. On the other hand, the generated trajectories rely on propulsion and aerodynamics models developed with accurate aircraft performance data derived from Airbus Performance Engineering Program (PEP). For the atmosphere, the International Standard Atmosphere (ISA) model is referred [24].

In order to guarantee a feasible trajectory, as a result of the optimization process, several constraints must be considered. For instance, the dynamics of the system or generic box constraints on the state and control variables (such as maximum and minimum operating speeds or flight path angles). The remaining constraints of the problem are specified by means of a flight profile. The flight profile is characterized in several user-defined phases, where different path constraints and event constraints may apply reflecting typical ATM practices and operational procedures.

The trajectory generation tool imposes constant Mach, IAS or altitude phases by means of optimization parameters that are bounded with the upper and lower values specified in the flight profile. It should be noted that the optimization algorithm will choose the (optimal) values of the different IAS, Mach and altitude phase dependent parameters, as well as the number of step climbs (if any) to perform. In addition, the solution might satisfy some algebraic event constraints fixing the initial and final conditions of the problem.

B. Simulation of the four Cases of study

In this paper, the flight profile is divided into several segments where different models and standard operational procedures apply. Fig. 5 summarizes the different segments and the corresponding path and event constraints, being m the step climb index. Taking this flight profile as baseline, the nominal flight and the three SR strategies presented in II could be simulated with the in-house tool presented above by properly configuring the input parameters as follows.

Case-0: the objective of the optimization is minimizing the cost function consisting of fuel F_i and time T_i, with different CI values, as Eq. 3, while satisfying the optimisation constraints that model current operational procedures (see details about nominal trajectory generation in [23]).

$$min(\sum F_i + CI \cdot T_i), \forall i \in [CL_1, \cdots, DE_4] \qquad (3)$$

where CL_1 and DE_4 are, respectively, the first climb and the last descent segments as shown in Fig. 5.

From Case-1 to Case-3, the fuel consumption for the whole flight is constrained to the same (or lower) that obtained in the nominal flight (Case-0), as depicted in Eq. 2, while the cost function becomes the total flight time, which is to be maximized (see Eq. 1).

Since typically the cruise speed is constant Mach number, in order to realize the SR in practice, an extra segment is added in front of each cruise phase allowing speed changes (see SR_1, SR_{m+1} in Fig. 5), as well as a similar segment (SR_{m+2}) at the end of the last cruise phase to achieve the optimal descent Mach.

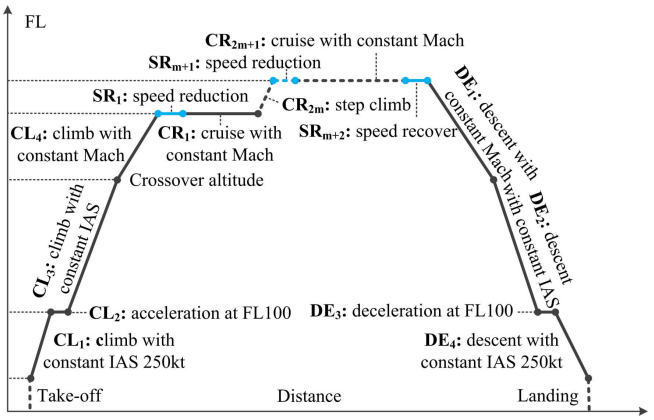

Fig. 5. Simulated flight profiles, divided into specific segments.

Note: the dash line in cruise phase means possible step climb cruise, which could be more than once if cruise is long enough. The subscript m is the ordinal number of the step climb cruise and equals to 0, 1, , n.

Case-1: the SR is implemented only in cruise phase. In other words, the optimization process only considers segments between SR_1 and SR_{m+1} (inclusive), being the climb and descent phases fixed to those of the nominal flight. Therefore, only the cruise speed is subject of optimization. In addition, the following event constraints must be enforced at both initial and final points of each step climb segment CR_{2m} (if any), in order to preserve the vertical profile of the nominal cruise phase:

$$H^{CR_{2m}}_{Case-1} = H^{CR_{2m}}_{Case-0}, D^{CR_{2m}}_{Case-1} = D^{CR_{2m}}_{Case-0} \qquad (4)$$

where H and D denote the altitude and distance respectively.

Case-2: the SR is extended to include climb and descent phases but keeping unchanged the nominal cruise altitude (or altitudes if $m > 0$). Accordingly, the whole flight (from CL_1 to DE_4) is subject of optimization. The following event constraint must be enforced so that the altitude of both TOC (final point of CL_4) and TOD (initial point of DE_1) remain unchanged:

$$H^{CL_4}_{Case-2} = H^{CL_4}_{Case-0}, H^{DE_1}_{Case-2} = H^{DE_1}_{Case-0} \qquad (5)$$

Nevertheless, the distance at which each step climb (if any) is performed is no longer enforced, considering that possible changes in the TOC and/or TOD positions could impact on the length of the different cruise segments. It should be noted that the weight at the initial point of CL_1 is always fixed in order to avoid unrealistic shifts on the aircraft weight.

Case-3: the SR is implemented in the whole flight in the same manner as Case-2. In this case, however, only constraint of fuel consumption is enforced, allowing the solver to optimize also the cruise altitude (or altitudes).

TABLE I
ANALYZED FLIGHTS FOR AIRBORNE DELAY COMPARISON.

Flights		Case-0										Case-1		Case-2		Case-3		
		Nominal flight by PEP					Nominal flight by the in-house tool											
Routes	CI (kg/min)	FL (100 ft)	Cruise Dist (nm)	Cruise Time (min)	Flight Time (min)	Fuel Burn (kg)	FL (100 ft)	Cruise Dist (nm)	Cruise Time (min)	Flight Time (min)	Fuel Burn (kg)	AD (min)	AD (%)	AD (min)	AD (%)	FL (100 ft)	AD (min)	AD (%)
FCO-CDG (595 Nm)	**25**	380	346	46	89	3428	380	345.82	46.58	89.28	3464	7.67	16%	21.70	24%	380	21.70	24%
	60	360	373	49	87	3573	380	345.11	45.57	86.33	3575	12.03	26%	25.80	30%	340	33.95	39%
	100	380	331	43	87	3599	380	337.97	44.35	85.47	3641	10.23	23%	29.28	34%	340	36.90	43%
	150	360	363	47	86	3640	380	338.64	44.37	85.35	3654	9.75	22%	29.63	35%	320	38.33	45%
	300	300	419	53	85	3945	300	378.00	48.17	83.47	3991	11.63	24%	52.75	63%	260	55.33	66%
	500	260	446	56	84	4266	260	424.58	53.17	82.58	4302	23.12	43%	60.12	73%	260	60.12	73%
AMS-SVQ (1000 Nm)	**25**	380	741	99	144	5443	380	728.76	98.08	143.82	5482	16.33	17%	34.97	24%	380	34.97	24%
	60	380	733	96	140	5609	380	726.75	96.00	139.73	5640	24.43	25%	44.15	32%	360	50.95	36%
	100	380	720	94	140	5683	380	702.39	91.97	138.12	5768	21.42	23%	48.75	35%	340	59.57	43%
	150	340	783	101	138	5906	340	754.33	97.83	136.93	5974	22.35	23%	70.92	52%	320	71.72	52%
	300	300	819	104	136	6365	300	772.25	98.38	135.12	6389	24.75	25%	89.58	66%	280	90.37	67%
	500	260	847	106	134	6988	260	824.27	103.23	133.38	6998	43.88	43%	103.87	78%	260	103.87	78%
STO-ATH (1305 Nm)	**25**	360	255	34	184	7003	360	40.36	5.45	185.00	7054	0.47	9%	41.67	23%	360	41.67	23%
		380	785	105			380	991.46	133.45			23.23	17%			380		
	60	360	184	24	180	7208	360	40.33	5.32	180.17	7242	1.30	24%	62.28	35%	360	62.28	35%
		380	845	111			380	988.04	130.57			36.50	28%			380		
	100	380	1009	132	180	7299	380	997.35	130.58	178.17	7360	30.93	24%	61.47	34%	360	71.28	40%
	150	340	1082	140	178	7361	340	1050.44	136.23	176.60	7467	51.30	38%	83.23	47%	320	85.60	48%
	300	300	1119	142	175	7579	300	1069.47	136.27	174.08	7830	58.52	43%	109.87	63%	280	109.97	63%
	500	260	1148	144	173	9057	260	1125.73	141.00	171.72	9159	58.97	42%	126.22	74%	260	126.22	74%

IV. ILLUSTRATIVE EXAMPLES

In this section, some specific routes are analysed in detail: Rome to Paris (FCO-CDG: 595nm), Amsterdam to Seville (AMS-SVQ: 1000nm) and Stockholm to Athens (STO-ATH: 1305nm). All of them are representative of short and mid haul flights in Europe. Each route is further analysed with different CI ranging from 25 to 500kg/min. Airbus A320, a common two-engine narrow-body transport aircraft is the research object for this paper.

Four cases, from Case-0 to Case-3, are all included. Case-0 is conducted twice, one from PEP (Airbus Performance Engineering Programs) and the other from the in-house trajectory generation tool presented in Sec. III-A. The idea is to validate this tool, comparing its results with the PEP ones. Since PEP cannot simulate SR strategies, Case-1 to Case-3 are all produced by using the in-house tool.

Some assumptions have been taken in this experiment: 1) Great Circle Distance (GCD) is considered between origin and destination airports, instead of considering air traffic services routes; 2) a passenger occupation (payload factor) of 81% is considered for all flights [6]; 3) no wind conditions are considered; 4) alternate and reserve fuel are not included; 5) only even flight levels are used (FL260 as the lowest altitude); and 6) cruise step climbs are allowed with 2000ft steps and 5 minutes as minimum time for each flight level.

A. Airborne delay comparison

Results are summarized in Table I. The results for Case-0 corroborate the accuracy of the performance model, since both PEP and the in-house tool present similar fuel consumption and flight profiles. The small differences observed might be due to the errors in the function fitting process of the performance data and truncation effects. Nevertheless, considering that most of the differences are within the scope of 1%-2%, we believe that for this paper the results are acceptable. Once the trajectory generation tool is validated, it could be appropriate to conduct the remaining simulations from Case-1 to Case-3.

With respect to Case-1, we observe similar results as those found in our former work, which were based on PEP (see more details in [6]).

As for Case-2, the air delay caused by SR increases significantly only after climb and descent phases are included. If we compare the percentage that climb and descent normally account for in a flight, with the percentage that cruise has, we may find that for those short-haul flights, the distances of climb

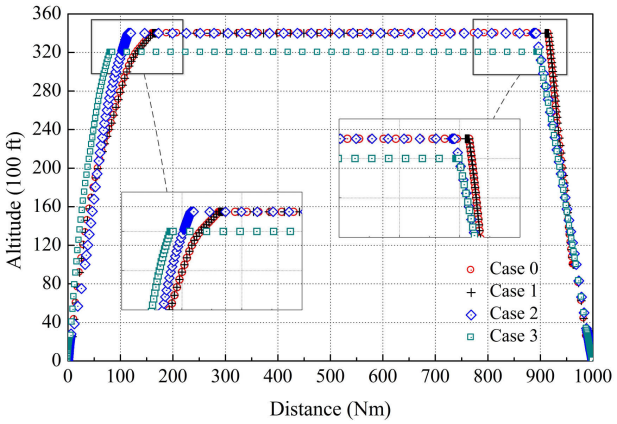

Fig. 6. Optimal trajectories generated for each Case.

TABLE II
DETAILS OF A SPECIFIC FLIGHT FROM CLIMB, CRUISE AND DESCENT POINTS OF VIEW.

Cases	Climb phase				Cruise phase						Descent phase				Total	
	Fuel (kg)	Time (min)	Dist (nm)	Avg speed (kt)	FL (100ft)	Fuel (kg)	Time (min)	Dist (nm)	Specific range (nm/kg)	Avg speed (kt)	Fuel (kg)	Time (min)	Dist (nm)	Avg speed (kt)	Fuel (kg)	Time (min)
Case 0	1685.43	21.55	157.31	437.98	340	4006.53	97.83	754.33	0.188	462.62	107.19	12.62	75.63	359.67	5799.15	132.00
Case 1	1685.43	21.55	157.31	437.98	340	4006.53	120.18	754.33	0.188	376.59	107.19	12.62	75.63	359.67	5799.15	154.35
Case 2	1415.80	23.30	110.70	285.06	340	4199.83	156.78	777.10	0.185	297.39	183.52	22.83	99.48	261.42	5799.15	202.92
Case 3	1064.42	13.67	76.38	335.33	320	4558.76	168.52	818.11	0.179	291.29	175.97	21.53	92.79	258.53	5799.15	203.72

and descent may account for up to 50% while time nearly 50% too, but for the mid/long-haul flights, both distance and time percentages could reduce to about 20%. Nevertheless, most of the air delay in Case-2 increase to almost 3-fold of the ones in Case-1, which is unexpected and interesting to see the possible reasons. In addition, these striking results demonstrate that significant airborne delay could be absorbed without requiring modifications in the flight plan, which contains information about the planned route and cruise flight levels.

Finally, when the cruise flight level is allowed to change, as Case-3, the air delay further increase but not so remarkable as from Case-1 to Case-2 (see Table I). for these low cruise speeds, the SR curves for different cruise flight levels are quite close. As a result, the speed reduction from altitude changes, i.e., Case-2 to Case-3, will not be as large as the reduction from nominal speed to equivalent speed, i.e., Case-1 to Case-2. Typically, the new flight level would be lower than the original, but since the step interval is 2000ft, which is a discrete change due to operation constraints, some flights just keep unchanged as Case-2.

B. Analysis for a specific flight: AMS-SVQ with CI=150

In order to better illustrate how the SR strategy affects the trajectory profiles for each considered Case of study, the AMS-SVQ: CI=150 flight (see I) is analysed in detail. The vertical trajectories corresponding to the four Cases are shown in Fig. 6. The changes when SR is implemented in climb and descent phases can be appreciated in the profile, while the optimal flight level for Case-3 decreases from FL340 to FL320. Comparing the blue dots (Case-2) with the red ones (Case-0), we find the aircraft is climbing steeper (recall that the cruise flight level keeps unchanged for this Case), saving some fuel while delaying the flight. Conversely, the descent is performed more gradually and flying slower, but burning some extra fuel if compared with Case-0. As for the green squares (Case-3), a decrease in cruise flight level generates even steeper climb and shallower descent trajectories. Table II illustrates clearly these changes for all Cases of study.

Compared with the nominal flight (Case-0), Case-1 consumes the same amount of fuel in each phase and achieves 22 minutes of airborne delay when cruising, which accounts for the 22% of the cruise time and the 17% of the total time.

In Case-2, the fuel consumption reduces 270kg (16%) in climb and the airborne delay is almost 2 minutes in this phase. Since the total fuel consumption is the same for the flight, the 270kg of fuel saved in climb can actually be allocated in cruise (193kg, 5% of cruise) and descent (77kg, 71% of descent), which, in fact, allows to largely increase the time delayed in both phases: 59 minutes (60% of cruise) and 10 minutes (77% of descent), respectively. As a result, if we compare Case-2 with Case-1, it seems that a 193kg (5%) increase of fuel consumption in cruise could exchange for 37 minutes (31%) more time delayed.

Regarding Case-3, when cruise flight level is allowed to change, the new optimal altitude (FL320) allows the aircraft to perform even more airborne delay with the same fuel consumption than in Case-0 (nominal Case). Compared to Case-2, 351kg (25%) of fuel are saved during the climb phase, 8kg (4%) of fuel during the descent phase, and 359kg (9%) of fuel are added to the cruise phase, lowering the specific range by 0.006 nm/kg, and further reducing the equivalent cruise speed to produce an even longer (12 minutes) air delay in cruise. Although the flight time in both climb and descent are shorter, the total flight time increases (by 1 minute) due to this extended cruise flight time.

As we can tell from Fig. 7(a), the climb speed profiles of all the Cases have quite similar structures, which mainly include a continuous acceleration process at low altitude, a constant IAS climb, followed by constant Mach climb at higher altitudes. At the end of the climb a small deceleration is observed in order to reach the (reduced) optimal cruise speed. Making Case-0 as the baseline, the difference with Case-1 only lies on the deceleration process at cruise flight level, so they share exactly the same climb speed V_0^{clb}. Note that the speed in the climb phase changes in different periods, so we simply assume the average IAS speed as the climb speed, while the same assumption on descent speed.

In Case-2 when SR is allowed in climb (and descent), the optimizer chooses a climb speed around 210kt (instead of the 300kt observed in Case-0). This new speed is in fact the minimum speed allowed (GD speed). Due to this lower IAS climb, a higher crossover altitude (around FL320) is obtained to change to the climb Mach number, which is also lower than the nominal one. According to our discussions in Section. II, if the climb speed had reduced to V_{eq}^{clb}, the fuel consumption would have been 1685kg, as in Case-0. However, the lower speed bound is set to V_{GD}^{clb}, which is higher than V_{eq}^{clb} for this particular case (see 7(b)). For this Case this V_{GD}^{clb} speed leads to 1415kg of fuel consumption in climb (see Table II).

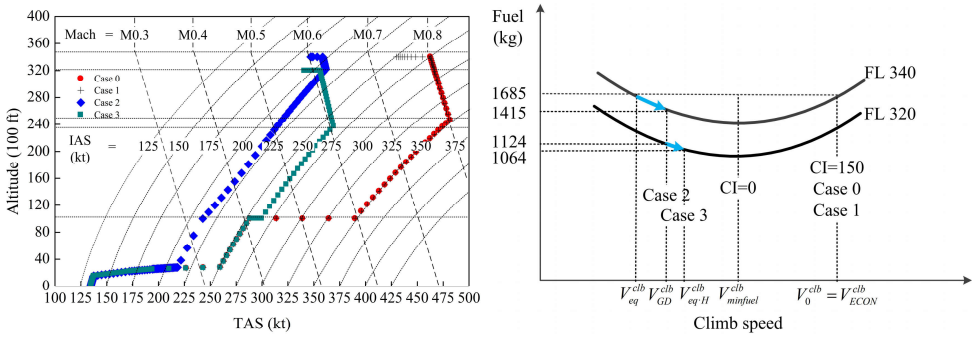

(a) Speed profile (b) Fuel consumption

Fig. 7. Differences in speed and fuel for all the four Cases with respect to the climb phase.

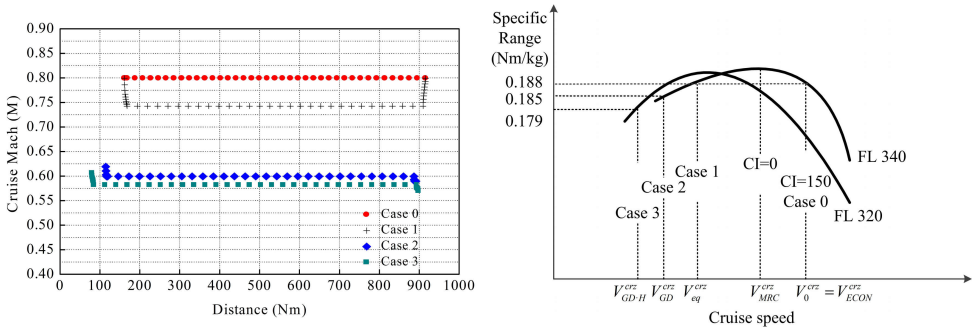

(a) Speed profile (b) Specific range

Fig. 8. Differences in speed and specific range for all the four Cases with respect to the cruise phase.

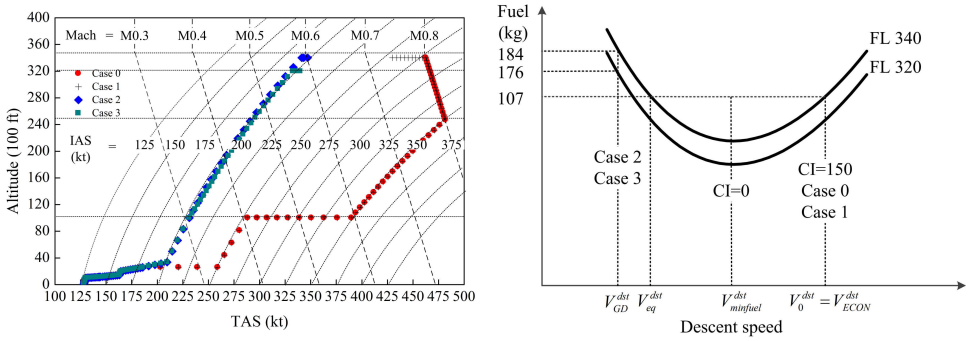

(a) Speed profile (b) Fuel consumption

Fig. 9. Differences in speed and fuel for all the four Cases with respect to the descent phase.

Recall that it is the total fuel consumption that we keep unchanged, not climb, cruise or descent fuel consumptions separately (see Eq. 2). Therefore, the SR in cruise or descent phase could take advantage of the saved fuel in climb to produce even more airborne delay.

In Case-3, results show that the climb speed is set to V_{eqH}^{clb}, higher than the GD speed used in Case-2 (see Fig. 7(a)). The climb speed increases from V_{GD}^{clb} to V_{eqH}^{clb}, as shown the blue line in Eq. 7(b), while the gained fuel makes a longer delay time in cruise and descent phases since the total flight time is longer than Case-2 (see Table II). That means, in this case, part of the delay time is trade in exchange for saving more fuel.

When it comes to the cruise phase, if the fuel consumption is fixed in this phase in Case-1, then the cruise Mach decreases from M0.8 to M0.74, while the specific range keeps the same (both 0.188nm/kg). Unlikely, in Case-2 and Case-3, the cruise Mach both reduce directly to the GD speed for each flight level, M0.6 and M0.58 respectively (see Fig. 8(a)). The added 193kg fuel in cruise phase of Case-2 leads to a decrease in specific range from 0.188nm/kg to 0.185nm/kg. If the curve of specific range becomes flatter when speed is lower than V_{eq}^{crz},

it happens that a slightly decrease in specific range could bring a relative larger decrease in the cruise speed, as shown in Fig. 8(b). Considering the long distance and time that cruise phase takes, this decrease in speed may produce a remarkable amount of airborne delay: 37 minutes more than Case-1. In addition, the added distance in cruise also helps to extend delay time in cruise phase, which equals to 23nm in Case-2 and 49nm in Case-3 respectively.

As for the descent phase, we can see from Fig. 9(a) that Case-2 and Case-3 have no deceleration below FL100 (like in Case-0 and Case-1) simply because the descent speed (around 200kt) is already below the ATC constraint of IAS lower than 250kt below FL100. Meantime, the segments of constant Mach descent are both missing too, since the crossover altitudes lie higher above the cruise flight level due to the lower speed in the constant IAS descent in Case-2 and Case-3.

Normally, the fuel consumed in descent phase accounts for the lowest of the three phases, but the trade-off still generates almost double the descent time in our example (see Table. II). In Case-2, the fuel consumption grows from 107kg to 184kg, reducing the descent speed from V_0^{dst} to V_{GD}^{dst} which is the GD speed in descent. Remember that the GD speed is not the same in climb that in descent, since the weight of the aircraft is different (fuel has been burnt in cruise). In addition, results show that in Case-3 it chooses the GD speed as the same in Case-2, but consumes 176kg fuel less than 184kg in Case-2 (see Fig. 9(b)), due to the lower altitude of TOD.

V. Conclusions and future work

This paper extends previous research on linear holding strategies in cruise phases to absorb part of air traffic flow management delays by allowing speed reduction on climb and descent phases too. Three different variants are analysed and compared and maximum airborne delay trajectories are computed by means of numerical optimisation using an in-house trajectory optimisation tool, which relies on accurate performance models derived from manufacturer data.

Compared with previous works, a remarkable increase of the maximum airborne delay that can be realized without extra fuel consumption is observed. Compared with the speed reduction strategy only in the cruise phase, adding climb and descent makes it possible to re-allocate the fuel consumption in each phase, as long as the total fuel keeps unchanged.

Considering that the trade-off between fuel and time exists in every phase but varies between each phase, which is also dependent on factors such as altitude, weight, etc., the optimal trajectory generation tool could help to find the best solution that produces the longest airborne delay.

Further work will aim to explore the effects of this SR strategy for the whole flight in realistic scenarios, as done for instance in [2], including taking wind factors into consideration as it always has great effects on real flights.

Acknowledgment

The authors would like to thank Airbus Industrie for the use of PEP (Performance Engineers Program) suite, which allowed us to undertake realistic aircraft performances simulations. This research is partially supported by grants from the Funds of China Scholarship Council (201506830050).

References

[1] L. S. Cook and B. Wood, "A model for determining ground delay program parameters using a probabilistic forecast of stratus clearing," *Air traffic control quarterly*, vol. 18, no. 1, p. 85, 2010.

[2] L. Delgado, X. Prats, and B. Sridhar, "Cruise speed reduction for ground delay programs: A case study for san francisco international airport arrivals," *Transportation Research Part C: Emerging Technologies*, vol. 36, pp. 83–96, 2013.

[3] M. O. Ball, R. Hoffman, and A. Mukherjee, "Ground delay program planning under uncertainty based on the ration-by-distance principle," *Transportation Science*, vol. 44, no. 1, pp. 1–14, 2010.

[4] T. R. Inniss and M. O. Ball, "Estimating one-parameter airport arrival capacity distributions for air traffic flow management," *Air Traffic Control Quarterly*, vol. 12, pp. 223–252, 2004.

[5] X. Prats and M. Hansen, "Green delay programs: absorbing atfm delay by flying at minimum fuel speed," in *Proceedings of the 9th USA/Europe air traffic management R&D seminar, Berlin, Germany*, 2011.

[6] L. Delgado and X. Prats, "En route speed reduction concept for absorbing air traffic flow management delays," *Journal of Aircraft*, vol. 49, no. 1, pp. 214–224, 2012.

[7] ——, "Operating cost based cruise speed reduction for ground delay programs: Effect of scope length," *Transportation Research Part C: Emerging Technologies*, vol. 48, pp. 437–452, 2014.

[8] ——, "Effect of wind on operating-cost-based cruise speed reduction for delay absorption," *Intelligent Transportation Systems, IEEE Transactions on*, vol. 14, no. 2, pp. 918–927, 2013.

[9] T. Günther and H. Fricke, "Potential of speed control on flight efficiency," in *2nd International Conference on Research in Air Transportation (ICRAT)*, vol. 1, 2006, pp. 197–201.

[10] A. Australia, "Annual report," Tech. Rep., 2007.

[11] H. Huang and C. J. Tomlin, "A network-based approach to en-route sector aircraft trajectory planning," in *AAIA Guidance, Navigation and Control Conference*, 2009.

[12] D. Bertsimas and S. S. Patterson, "The traffic flow management rerouting problem in air traffic control: A dynamic network flow approach," *Transportation Science*, vol. 34, no. 3, pp. 239–255, 2000.

[13] A. Lecchini, W. Glover, J. Lygeros, and J. Maciejowski, *Monte Carlo optimisation for conflict resolution in air traffic control*. Springer, 2006.

[14] H. Erzberger and L. Tobias, "A time-based concept for terminal-area traffic management," 1986.

[15] D. Knorr, X. Chen, M. Rose, J. Gulding, P. Enaud, and H. Hegendoerfer, "Estimating atm efficiency pools in the descent phase of flight," in *9th USA/Europe air traffic management research and development seminar (ATM2011)*, vol. 5, 2011, pp. 16–23.

[16] J. C. Jones, D. J. Lovell, and M. O. Ball, "En route speed control methods for transferring terminal delay," in *10th USA/Europe Air Traffic Management Research and Development Seminar (ATM2013), Chicago*, 2013.

[17] ——, "Combining control by cta and dynamic en route speed adjustment to improve ground delay program performance," 2015.

[18] B. Roberson and S. S. Pilot, "Fuel conservation strategies: cost index explained," *Boeing Aero Quarterly*, vol. 2, no. 2007, pp. 26–28, 2007.

[19] Airbus, *Flight Crew Operation Manual (FCOM). A320. Version 1.3.1*, 1993.

[20] ——, *Flight Crew Operation Manual (FCOM). A320. Version 1.3.1*, 1993.

[21] ——, *Flight Operations Support and Line Assistance: Cost index*, 1998.

[22] J. T. Betts, *Practical methods for optimal control and estimation using nonlinear programming*. Siam, 2010, vol. 19.

[23] R. Dalmau and X. Prats, "Fuel and time savings by flying continuous cruise climbs: Estimating the benefit pools for maximum range operations," *Transportation Research Part D: Transport and Environment*, vol. 35, pp. 62–71, 2015.

[24] I. C. A. Organization, *Manual of the ICAO Standard Atmosphere: Extended to 80 Kilometres (262 500 Feet)*. International Civil Aviation Organization, 1994.